

Application of Artificial Intelligence in Single Point Incremental Forming for Surface Roughness Prediction

Ranjeet Prasad¹, Manish Oraon^{2,*}, Vinay Sharma³

Abstract

The sheet metal forming industries always try to find an emerging trend to form sheet-metal in a cost-effective manner. In this regard, a forming technique is trending termed as single point incremental forming (SPIF) in which a simple forming tool having hemispherical end rod is moving and simultaneously deforming the clamped metal sheet according to predetermined toolpath command and forms a complete shape. The achievement of required surface quality is difficult in the SPIF especially with the metals having low formability. To study the surface quality of SPIFed part, Cu-Zn alloy is taken for SPIF and conducted the experiments. In SPIF, statistically the step-depth size (Δz) and wall angle (θ) are found significant for surface roughness of CU-Zn alloy. In this paper, prediction model is established by using artificial intelligence where artificial neural network (ANN) model is established to predict the surface roughness virtually with the set inputs and measured output. The optimum 6-6-1 model is built with the segregation of experimental data into training (70%), testing (51%), and validation (15%). The overall co-efficient of regression (R^2) and mean absolute error (MAE) of the model is found 0.93219 (93.219%) and -1.37 respectively. It is confirmed that properly selected ANN model can be utilized as a prediction tool in manufacturing processes where the output responses always vary.

Keywords: SPIF, Input parameters, surface roughness, ANOVA, ANN

INTRODUCTION

In recent years, an effort has made the manufacturing industry to minimize the processing period and cost of production. The need of customized part, model, and production of small batch enunciate the techniques like rapid prototyping, 3D printing etc. These advanced technologies turn the raw materials into finished part in less time and minimum effort [1]. Accordingly, an advanced technique, known as Incremental sheet metal forming (ISMF), is developed to accelerate the forming industries. The flexible

processing of ISMF comprises higher complexity therefore an attention towards calibration of the process is required [2]. The spring-back effect was merely investigated as it is not observed excessively in small part formation, but it was tried to simulate through different techniques [3–4]. The construction of computational systems and algorithms is a basic science of artificial intelligence (AI) that can perform a variety of tasks such as learning, interpretation reasoning, decision making etc. [5–6]. In Manufacturing, AI has important applications in different areas such as process planning, quality control, predictive maintenance, optimization, logistic, etc. [7]. The technological principle of SPIF involves clamping the blank from its edges and progressively

*Author for Correspondence

Manish Oraon

¹ Research Scholar, Department of Production and Industrial Engineering, Birla Institute of Technology, Mesra, Jharkhand, India

^{2,3} Faculty, Department of Production and Industrial Engineering, Birla Institute of Technology, Mesra, Jharkhand, India

Received Date: January 06, 2024

Accepted Date: March 16, 2024

Published Date: May 04, 2024

Citation: Manish Oraon, Ranjeet Prasad, Vinay Sharma. Application of Artificial Intelligence in Single Point Incremental Forming for Surface Roughness Prediction. Journal of Polymer & Composites. 2024; 12(Special Issue 1): S237–S246p.

deforming it using a single hemispherical end rod as per input commands in computer numerical control (CNC) based machine. Researchers have proposed several approaches to SPIF, however strong results are still awaited. The main limitations of SPIF, such as longer process time, sheet thinning, and limited geometrical accuracy, hinder its wider industrial application [8]. Extensive investigations concentrated on the maximum forming of thin sheet of metal without failure and their optimization in ISMF. Industrial research primarily targets the geometric precision of forming parts, both at the macroscopic levels. An experimental-statistical analysis is conducted on calamine brass Cu67Zn33 to examine the roughness profile of the product. Earlier investigations has indicated that the deformation rate is important factor in the SPIF process [9–12]. Preliminary studies of SPIF on SPCC steel [13]. reveals that the finished parts exhibited spring back and dimensional inaccuracy when SPIF is done with varying wall angles that results a large-scale waviness in the formed part [14]. By decreasing the vertical step size, the surfaces transformed from wavy to strictly rough [15]. The non-contacted surface roughness measurements system was utilized to measure sectional microstructure, and thickness distribution in the SPIF of AL3003 (H14) at higher tool feed rate and higher tool rotational speeds [16]. Experimental campaigns were analysed on AA7075 alloy to draw conclusions regarding the influence of the said parameters [17–18]. The medical implants were successfully formed through SPIF [19]. It was observed that the reducing friction and achieving reduced level of roughness on the punch surface improved the interior surface of titanium sheets. The effects of tool diameter, along with other process parameters were investigated during SPIF on various Indian standard metals such as steel, stainless steel, and aluminium to analyse the surface roughness and microstructural transformation. It is observed that a larger tool end diameter of hemispherical end tool and higher spindle speed improved the desired goals [20]. The formability of stainless steel SS304 grade through SPIF was investigated by considering variations in tool end along with few process variables. Statistical analysis showed that vertical size increment i.e. step-depth size increment contributed significantly to surface roughness [21]. Further the gradient boosting regression tree (GBRT) is used to correlate the functional variables of SPIF on the output response for Al/SUS bimetal sheet. The authors reported severe cracks when SPIF was done with 10 mm tool end diameter while the refinement in the surface roughness was noticed with 20 mm tool end diameter and small step size of 0.15 mm [22]. Overall, these studies and investigations highlight the various aspects, parameters, and challenges involved in SPIF, keeping all these finding in mind, the artificial neural network (ANN) model is introduced in SPIF to predict the surface quality of formed part which is a prime concern.

SPIF INVESTIGATION

Taguchi-based optimization offers advantages over conventional optimization practices with a minimum number of experiments [23]. Unlike traditional methods, Taguchi optimization is more cost-effective. However, to address the limitation of optimizing only one characteristic, several modifications have been suggested [24]. These modifications aim to extend the Taguchi method to handle multi-objective problems, but these modifications increase the computational complexity of the optimization process. In the context of multi-objective optimization, a simple modification has been proposed. This modification, described in [25], introduces a multi-objective for individual trial of the Orthogonal Array (OA). By using these membership functions, the multi-performance objectives can be considered simultaneously during the optimization process. This modified approach enables Taguchi-based optimization to handle multi-objective problems without significantly increasing computational complexity. It provides a more comprehensive and efficient way to optimize multiple performance characteristics simultaneously, making it a valuable tool in engineering and optimization applications.

SPIF Experiments

The SPIF experiments is conducted on CNC vertical machine centre (Model: DT-110, Mikrotool Pvt. Ltd., Singapore) place in the modern manufacturing laboratory of production and industrial engineering department, BIT, Mesra. A dedicated SPIF fixture is designed and fixed it over the CNC's table. The lower and higher value of the SPIF parameters domains i.e. step-depth size (Δz) in mm, feed rate (f) in

mm/min, spindle speed (R) in RPM, wall angle (θ) in degree, sheet thickness (T) in mm, and density of lubricant (L) in kg/m^3 are taken. The numeric values of considered input parameters for SPIF experiment is tabulated in Table 1. The Cu-Zn alloy is taken as metal sheet and a square pyramid shape of given dimensions is formed in each test sample with the prescribed tool trajectory as in Figure. 1.

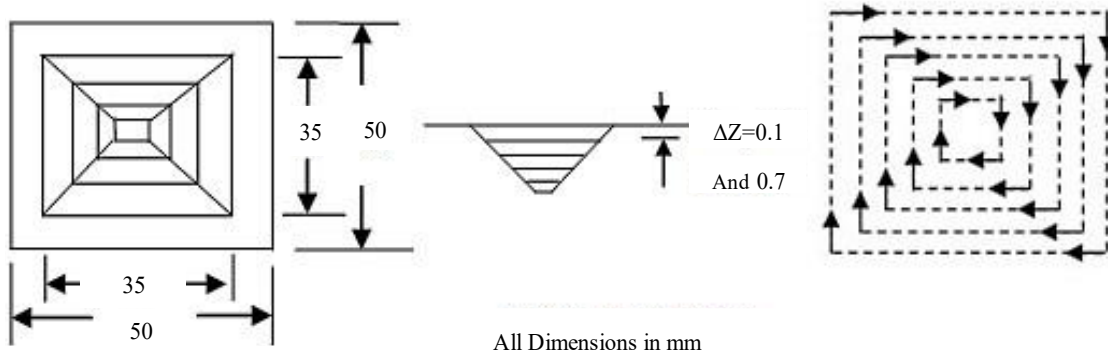


Figure 1. Proposed square pyramid shape and toolpath for forming.

The test sample is prepared by cutting 5mm*5mm from individual square pyramid for measuring the surface roughness measurement (See Figure. 2). Across the direction of tool movement as expected the waviness observed in the formed part due to continuous change in successive depth. The surface roughness of the cut sample of each experiment is measured in the magnification of 100X through atomic force measurement machine (AFM) (Model: NT-MDT, Solver-4) which is available in the central instrumentation facility-1 (CIF-1), BIT, Mesra, India.



Figure 2. AFM (Model: NT-MDT) Solver-4 used in surface roughness measurement.

The test sample piece is placed in the machine in such a way that optical probe scans the sample across the tool feed mark (due maximum surface roughness occur due to waviness). The optical probe scanned approximately 65000 grits in one pass and generated a 3D microscopic image along with average surface roughness (R_a), average heights of top ten peaks (R_y), and root mean square roughness (R_q). All the roughness values are measured in micron (μ) level. Only average surface roughness R_a is considered in the present study. The sample, cut section and AFM microscopic image of individual samples is presented in Figure. 3. The experiment set with varying level of input parameters along with measured R_a is tabulated in Table 1.

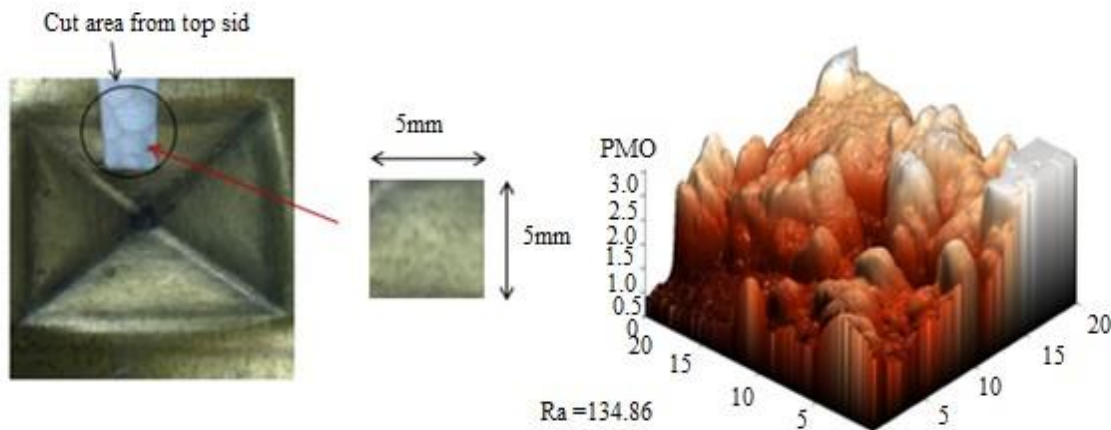


Figure 3. Sample Cut for AFM and microscopic image of a sample.

Statistical Analysis for Ra

In the present investigation, the significant input parameters on the output response, specifically the surface roughness (Ra) are being analyzed using statistical methods. The software used for this analysis is MINITAB version 17.0.1, a popular tool for statistical analysis. In this case, it is used to assess how the input variables affect the output factor Ra. The significance level chosen for the analysis of variance ANOVA is 95% confidence. This means that there is a 95% probability that any observed differences in the output response (Ra) are not due to random chance but are instead influenced by the variations in the input parameters. The significance level is often denoted by the symbol alpha (α), and in this case, it is set to 0.05 (5%). The lower Ra-value shows the improved surface finish of the product therefore ‘smaller is better’ approach is made during ANOVA test. The equation for ‘smaller is better’ is expressed by equation (1).

$$S/N_{(smaller\ is\ better)} = -10 \log -10 \log_{10} \left(SUM \left(\frac{Y^2}{n} \right) \right) \quad (1)$$

Table 1. Experiment Set As Per Orthogonal Array L₁₆ Along With Measured Ra.

| Exp. No. | $\Delta z (10^{-1})$ | F(10 ¹) | R(10 ²) | T(10 ⁻¹) | θ | L(10 ⁻¹) | Ra |
|----------|----------------------|---------------------|---------------------|----------------------|----------|----------------------|---------|
| 1 | 1 | 2 | 5 | 2 | 15 | 1.5 | 62.951 |
| 2 | 1 | 2 | 5 | 4 | 45 | 4.9 | 104.863 |
| 3 | 1 | 2 | 20 | 4 | 15 | 4.9 | 58.29 |
| 4 | 1 | 2 | 20 | 2 | 45 | 1.5 | 102.943 |
| 5 | 1 | 10 | 5 | 4 | 15 | 4.9 | 67.6545 |
| 6 | 1 | 10 | 5 | 2 | 45 | 1.5 | 100.514 |
| 7 | 1 | 10 | 20 | 2 | 15 | 1.5 | 51.8449 |
| 8 | 1 | 10 | 20 | 4 | 45 | 4.9 | 107.392 |
| 9 | 7 | 2 | 5 | 4 | 15 | 4.9 | 89.637 |
| 10 | 7 | 2 | 5 | 2 | 45 | 1.5 | 86.358 |
| 11 | 7 | 2 | 20 | 2 | 15 | 1.5 | 130.65 |
| 12 | 7 | 2 | 20 | 4 | 45 | 4.9 | 144.369 |
| 13 | 7 | 10 | 5 | 2 | 15 | 1.5 | 74.845 |
| 14 | 7 | 10 | 5 | 4 | 45 | 4.9 | 152.597 |
| 15 | 7 | 10 | 20 | 4 | 15 | 4.9 | 86.102 |
| 16 | 7 | 10 | 20 | 2 | 45 | 1.5 | 151.637 |

Artificial Neural Network Modeling

In manufacturing, the variation in the outputs is very common for repeated experiments. The inconsistency in the output response may arise from the full proofing of the conducted experiments. Moreover, the variation in the input parameters magnitude enhanced the estimation of conducted experiments. To correlate the results, the prediction of output needs to be analyzed in such a manner so that the error on the product should be minimized [26]. Artificial Intelligence (AI) is a widely utilized tool in many sectors and set a benchmark [27–29]. Artificial Neural Network (ANN) is a module of AI utilized as predictor tool in various sectors such as manufacturing processes, healthcare, finance, sports, etc. to model the nonlinear functions into a reliable output [30-31]. In the continuing SPIF investigation ANN estimated that the deformation velocity rate, element size, and mass scaling as 16.49m/s, 1mm*1mm, and 19.01 respectively to minimize pillow effect [32]. With the insight knowledge of ANN, the present investigation is done on MATLAB version 7.10.0.499 (Math works Inc., U.S.A) where Levenberg- Marquardt algorithm is utilized. The 6-6-1 network topology as shown in Fig. 4 is developed. The experimental numeric codes of input parameters and the measured output response i.e. Ra is taken as inputs for the prediction of Ra.

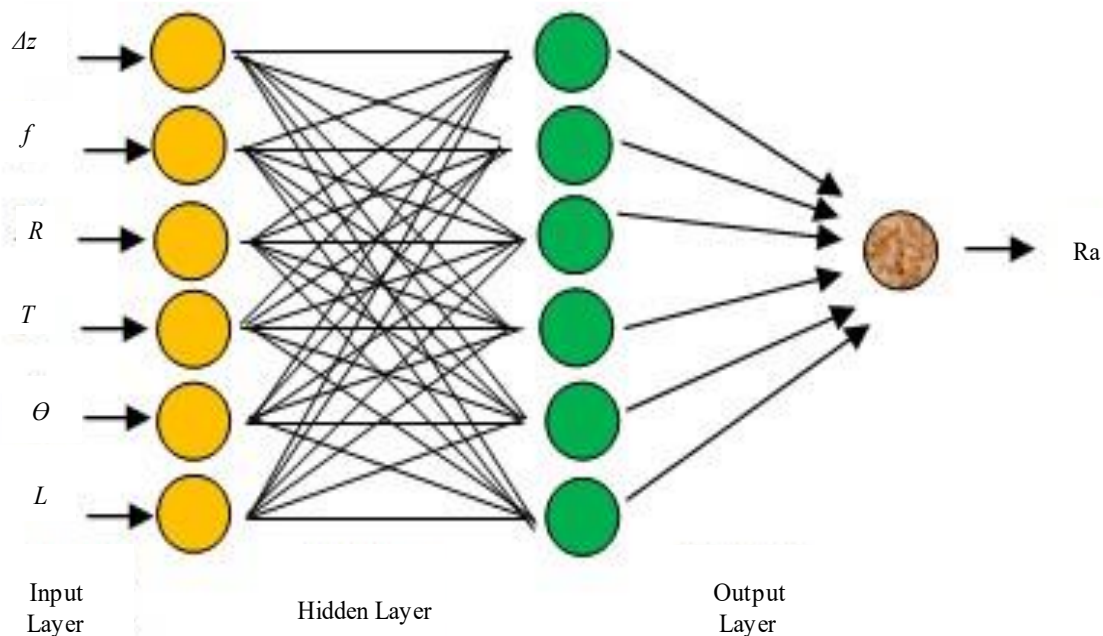


Figure 4. ANN Network Architecture 6-6-1 for Ra

According to Figure. 4, net input to unit ‘k’ in the hidden layer for single layer feed forward network is expressed in equation (2),

$$net_hidden = \sum_{j=1}^j wt_{j,k}i_j + bs_k \quad (2)$$

Where $wt_{j,k}$ is the weight. bs_k are the biases, and i_j is the inputs value. Now, the net input (for unit z) received is expressed in equation (3),

$$net_output = \sum_{k=1}^k v_{k,z}h_k + c_z \quad (3)$$

Where $v_{k,j}$ is the weight, c_z is the biases, and h_k is the outputs value at hidden nodes. After equating equations (2) and (3), the output at hidden and output nodes can be written as. equation (4) and equation (5) are the net information communicated to next layer for further analysis.

$$h_k = f(\text{net_hidden}) \tag{4}$$

$$o_z = f(\text{net_output}) = R_a \tag{5}$$

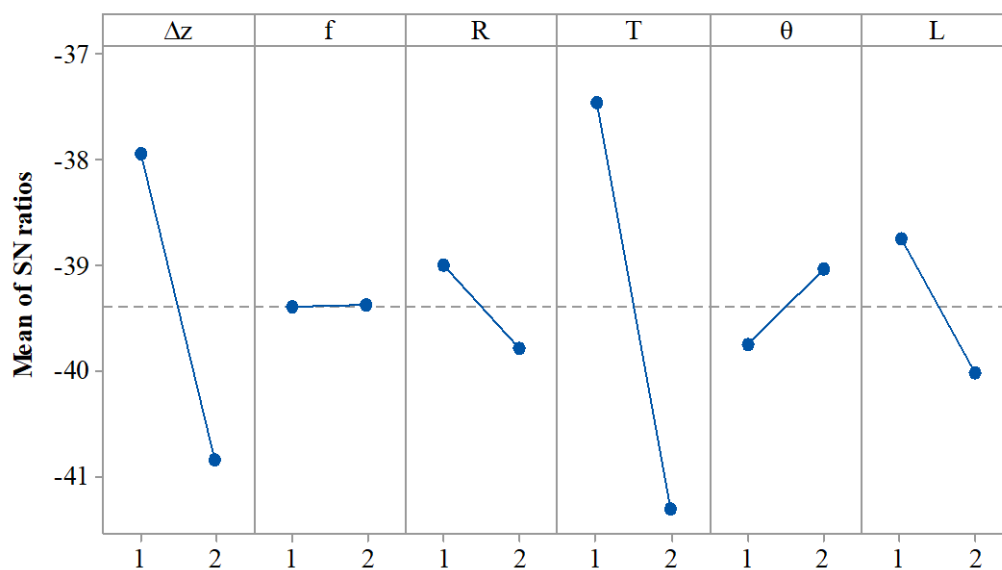
Where h_k is the net information transferred from input layer to hidden layer whereas o_z is the net information transferred to output layer.

The variety of ANN model is tested to get the best functional model for the prediction of Ra of SPIFed part. The ANN architecture is classified into three sections as shown in Table 3. In section 1, the transfer function TANSIG and at output layer, PURELIN transfer function is used. Similarly, section 2 is modeled by introducing LOGSIG at hidden layer whereas PURELIN transfer function at output layer and in the last section e.g. section 3, PURELIN transfer function in introduced at both hidden and output layers respectively. All the models are run by varying neurons e.g. 10, 11, and 12 neurons to find record the behavioral change of the ANN model. The feed forward backpropagation neural network (FFBP) in which Levenberg Marquardt (LM) training algorithm and LERNGDM learning rate are adopted for simulation of all the NN models. The mean square error (MSE) is the target which is further considered to confirm the reliability of the NN model.

RESULT AND DISCUSSION

The statistical analysis is done with 95% confidence level in which the probability factor (P) must be less than 0.05 shows the significance of individual input parameters. It is found step depth (Δz) and forming angle (θ) are the significant process parameters for the Ra-value in the SPIF of Cu67Zn33 alloy. Analysis of variance (ANOVA) results shows graphically in Figure. 5 where slopes of individual input parameters are drawn. The low level of input variables $\Delta z - f - R - T - L$ whereas $\theta = 45^\circ$ must be set in the SPIF of Cu67Zn33 alloy. Table 2 indicated that the step depth Δz (P=0.007) and wall angle θ (P= 0.001) are the significant.

Main Effects Plot (data means) for SN ratios



Signal-to-noise: Smaller is better

Figure 5. Main effect plot of individual input parameters

Table 2. Significance of Input Parameters For Ra Shown In Anova.

| Source | DF | Seq SS | Adj SS | F | P | Significance |
|----------------|----|---------|---------|-------|-------|--------------|
| Δz | 1 | 33.739 | 33.7493 | 11.85 | 0.007 | Yes |
| f | 1 | 0.003 | 0.0027 | 0.00 | 0.976 | No |
| R | 1 | 2.506 | 2.5063 | 0.88 | 0.373 | No |
| θ | 1 | 59.226 | 59.2263 | 20.79 | 0.001 | Yes |
| T | 1 | 2.006 | 2.0061 | 0.70 | 0.423 | No |
| L | 1 | 6.462 | 6.4623 | 2.27 | 0.166 | No |
| Residual Error | 9 | 25.641 | 25.6409 | | | |
| Total | 15 | 129.594 | | | | |

In ANN modeling, the input data are divided into 70% for training, 15% for testing and validation. The maximum numbers of iteration (first activated) and sufficient accuracy i.e. two stopping criteria is adopted during training of NN models. The network architecture generated by NN tool for the best possible solution is shown in Figure 6.

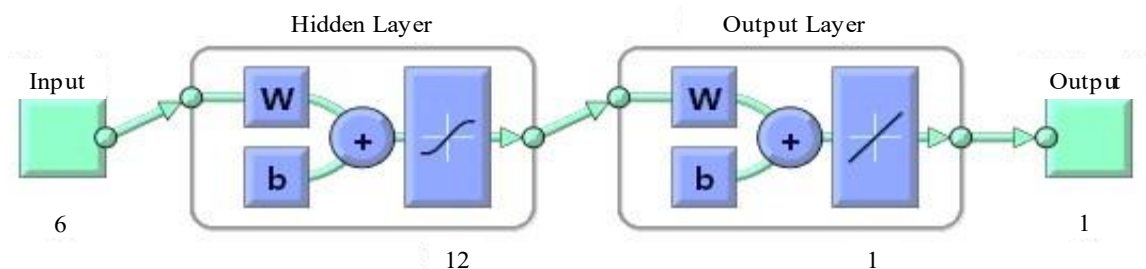


Figure 6. Main effect plot of individual input parameters

The Ra-value is predicted by using various ANN models in which neurons at hidden layer and type of transfer functions were varied. The training stopped at fifth iterations (first activated) with the value of 250.2109. The overall regression plot i.e. training, testing, and validation for the best possible NN solution are shown in Figure. 7. It seems that the input data for NN is to track the targets reasonably well.

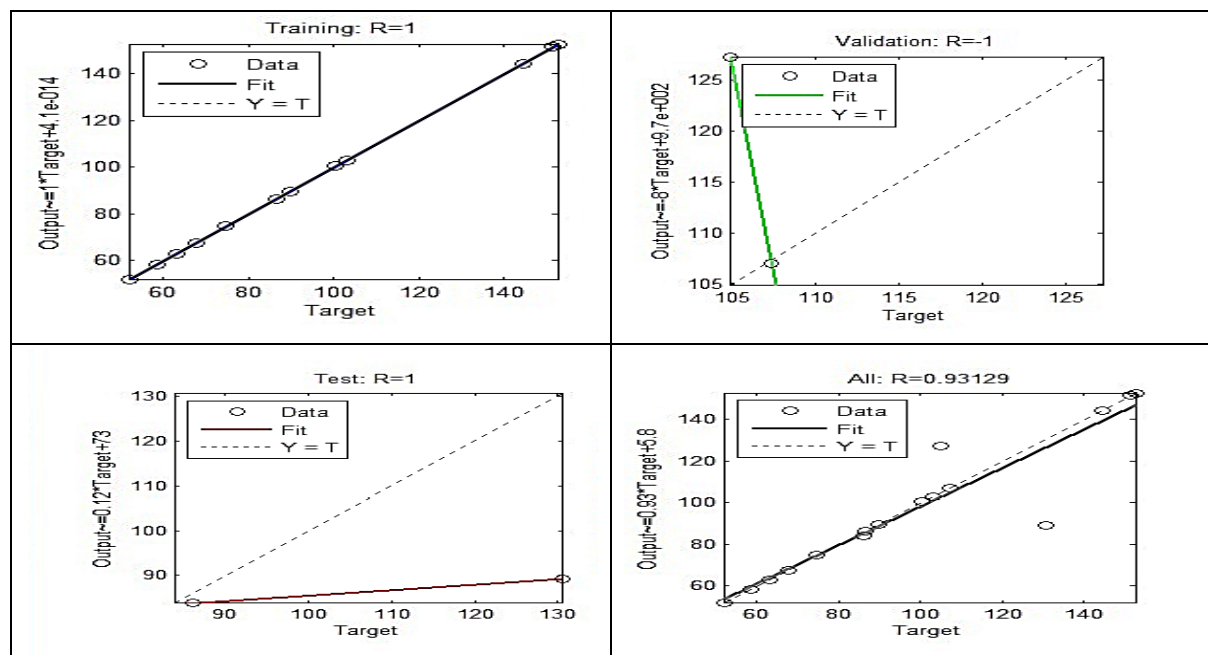


Figure 7. BPNN regression plot for Best NN model

Table 3 indicates the coefficient of correlation (CoC) for all the tested models are quite acceptable since the CoC for training, testing, and validation are more than 0.85 in most of the cases. To select the best ANN, the optimized CoC of 0.93219 with MSE of -5.34517 are reported in 6-12-1 NN where TANSIG at hidden layer and PURELIN at output layer. The training, testing and validation CoC's are reported as 1 for all and 0.93129 is overall CoC for the same NN model (Section 1 in Table 3). It seems that the input data for NN modeling tracked the targets reasonably well.

Table 3. Results of Ann for Targeted Ra And Predicted Ra With Mean Square Error.

| | Hidden layer neuron | Transfer function | | R ² | | | | MSE |
|-----------|---------------------|-------------------|---------|----------------|---------|------------|---------|-----------|
| | | Layer 1 | Layer 2 | Training | Testing | Validation | All | |
| Section 1 | Source | TANSIG | PURELIN | | | | | |
| | 10 | | | 1 | 0.99492 | 0.98472 | 0.91622 | -4.02081 |
| | 11 | | | 1 | 0.93854 | 0.99923 | 0.92942 | -3.04E-06 |
| | 12 | | | 1 | 1 | 1 | 0.93129 | -1.37 |
| Section 2 | | LOGSIG | PURELIN | | | | | |
| | 10 | | | 1 | 0.92499 | 0.40038 | 0.80506 | -2.87172 |
| | 11 | | | 1 | 0.86778 | 0.999981 | 0.77228 | 21.92478 |
| | 12 | | | 1 | 0.99612 | 0.88539 | 0.83074 | 1.090619 |
| Section 3 | | PURELIN | PURELIN | | | | | |
| | 10 | | | 0.91219 | 0.99238 | 0.98255 | 0.82366 | -6.90808 |
| | 11 | | | 0.92581 | 0.9993 | 0.96385 | 0.84981 | 1.249844 |
| | 12 | | | 0.96902 | 0.99541 | 0.94326 | 0.85703 | 5.609581 |

The correlation between predicted and actual response indicated by R_a -value which is in the range of 0 to 1.0. In the study, the lowest MSE value is observed for optimum ANN network. The combination of TANSIG with PURELIN in ANN is found most efficient than other combinations to get accurate results. Table 4 shows the comparative LM algorithm performance which is compared with measure R_a with MSE.

Table 4. Comparative R_a Along with MSE for best FFBP model

| Exp. No. | Experimental $R_a(\mu)$ | Predicted $R_a(\mu)$ | Error (MSE) |
|----------|-------------------------|----------------------|-------------|
| 1 | 62.951 | 62.951 | 0 |
| 2 | 104.863 | 127.2294 | 0 |
| 3 | 58.29 | 58.29 | 0 |
| 4 | 102.943 | 102.943 | 0 |
| 5 | 67.6545 | 67.6545 | 0 |
| 6 | 100.514 | 100.514 | 0 |
| 7 | 51.8449 | 51.8449 | 0 |
| 8 | 107.392 | 106.9841 | 0 |
| 9 | 89.637 | 89.637 | -2.13E-14 |
| 10 | 86.358 | 86.358 | -22.3664 |
| 11 | 130.65 | 89.30209 | -2.84E-14 |
| 12 | 144.369 | 144.369 | 1.42E-14 |
| 13 | 74.845 | 74.845 | 1.42E-14 |
| 14 | 152.597 | 152.597 | 0 |
| 15 | 86.102 | 83.91287 | -1.42E-14 |
| 16 | 151.637 | 151.637 | 0.40794 |

CONCLUSIONS

The surface roughness of the end part is examined and simultaneously analyzed the significance of input parameters. The prediction model is developed through ANN and feed forward back propagation method is utilized to enlighten the feasibility of AI tool in manufacturing processes. A few concluding points of the present study are mentioned below.

- The R_a -value of calamine brass can be improved by conduction SPIF at low step depth Δz along with greater wall angle.
- The optimum design for SPIF corresponds to $\Delta z=0.1\text{mm}$, $f=100\text{mm/min}$, $R=500$, $T=0.2\text{mm}$, $\theta=45^\circ$, and $L=15\text{Kg/m}^3$.
- The 6-12-1 model with TANSIG at hidden layer and PURELIN at output is found appropriate for predicting R_a .
- The CoC of 0.94855 is noticed resembles good agreement between input and output.
- ANN results found good agreement with experimental data where CoC found 0.94855 with MSE of -5.34517.

It is inferred that the output response is efficiently predicted through ANN. The benefit of using ANN included economic, approximate predictability, short simulation time which makes it a promising modelling tool. ANN could benefit industries in research and development activities.

Acknowledgments

The authors acknowledge the department of production and industrial engineering, BIT Mesra for their support and gratitude to FIST-II project sponsored by the department of science and technology, GOI.

REFERENCES

1. Porteus EL. Optimal Lot Sizing, Process Quality Improvement and Setup Cost Reduction. *Oper Res.* 1986;34(1):137-144.
2. Jeswiet J, Micari F, Hirt G, Bramley A, Duflou J, Allwood J. Asymmetric single point incremental forming of sheet metal. *CIRP Ann - Manuf Technol.* 2005;54(2):88-114.
3. Gomes C, Onipede O, Lovell M. Investigation of springback in high strength anisotropic steels. *J Mater Process Technol.* 2005;159(1):91-98.
4. Hai, T., Ali, M. A., Dhahad, H. A., Alizadeh, A. A., Sharma, A., Almojil, S. F., ... & Wang, D. (2023). Optimal design and transient simulation next to environmental consideration of net-zero energy buildings with green hydrogen production and energy storage system. *Fuel*, 336, 127126.
5. Leo Kumar SP. State of The Art-Intense Review on Artificial Intelligence Systems Application in Process Planning and Manufacturing. *Eng Appl Artif Intell.* 2017;65:294-329.
6. Pham DT, Afify AA. Machine-learning techniques and their applications in manufacturing. *Proc Inst Mech Eng Part B J Eng Manuf.* 2005;219(5):395-412.
7. Sharma, A., Sharma, K., Islam, A., & Roy, D. (2020). Effect of welding parameters on automated robotic arc welding process. *Materials Today: Proceedings*, 26, 2363-2367.
8. Shim MS, Park JJ. The formability of aluminum sheet in incremental forming. *J Mater Process Technol.* 2001;113(1-3):654-658.
9. Ambrogio G, Cozza V, Filice L, Micari F. An analytical model for improving precision in single point incremental forming. *J Mater Process Technol.* 2007;191(1-3):92-95.
10. Bahloul R, Arfa H, Belhadjsalah H. A study on optimal design of process parameters in single point incremental forming of sheet metal by combining Box-Behnken design of experiments, response surface methods and genetic algorithms. *Int J Adv Manuf Technol.* 2014;74(1-4):163-185.
11. Sharma, A., Chaturvedi, R., Sharma, K., & Saraswat, M. (2022). Force evaluation and machining parameter optimization in milling of aluminium burr composite based on response surface method. *Advances in Materials and Processing Technologies*, 8(4), 4073-4094.
12. Park JJ, Kim YH. Fundamental studies on the incremental sheet metal forming technique. *J Mater Process Technol.* 2003;140(1-3 SPEC.):447-453.

13. Pohlak M, Majak J, Küttner R. Manufacturability and limitations in incremental sheet forming. *Est J Eng.* 2007;13(2):129. doi:10.3176/eng.2007.2.06
14. Chaturvedi, R., Sharma, A., Sharma, K., & Saraswat, M. (2022). Tribological behaviour of multi-walled carbon nanotubes reinforced AA 7075 nano-composites. *Advances in Materials and Processing Technologies*, 8(4), 4743-4755.
15. Hagan E, Jeswiet J. Analysis of surface roughness for parts formed by computer numerical controlled incremental forming. *Proc Inst Mech Eng Part B J Eng Manuf.* 2004;218(10):1307-1312.
16. Liu, Z., Zhanguo, S. U., Abed, A. M., Chaturvedi, R., Feyzbaxsh, M., & Salavat, A. K. (2022). A comparative thermodynamic and exergoeconomic scrutiny of four geothermal systems with various configurations of TEG and HDH unit implementations. *Applied Thermal Engineering*, 216, 119094.
17. Oraon M. Statistical analysis to predict the surface roughness in single point incremental forming of Cu67Zn33 alloy. *Int J Product Qual Manag.* 2020;31(4):593.
18. Hamilton K, Jeswiet J. Single point incremental forming at high feed rates and rotational speeds: Surface and structural consequences. *CIRP Ann.* 2010;59(1):311-314.
19. Durante M, Formisano A, Langella A. Comparison between analytical and experimental roughness values of components created by incremental forming. *J Mater Process Technol.* 2010;210(14):1934-1941.
20. Kumar, R., Pandey, A. K., Samykano, M., Mishra, Y. N., Mohan, R. V., Sharma, K., & Tyagi, V. V. (2022). Effect of surfactant on functionalized multi-walled carbon nano tubes enhanced salt hydrate phase change material. *Journal of Energy Storage*, 55, 105654.
21. Ham M, Jeswiet J. Single Point Incremental Forming Limits Using a Boxbehnken Design of Experiment. *Key Eng Mater.* 2007;344:629-636.
22. Abd Ali R, Chen W, Al-Furjan MSH, Jin X, Wang Z. Experimental Investigation and Optimal Prediction of Maximum Forming Angle and Surface Roughness of an Al/SUS Bimetal Sheet in an Incremental Forming Process Using Machine Learning. *Materials (Basel).* 2019;12(24):4150.
23. Liu Z, Liu S, Li Y, Meehan PA. Modeling and Optimization of Surface Roughness in Incremental Sheet Forming using a Multi-objective Function. *Mater Manuf Process.* 2014;29(7):808-818.
24. Cao, Y., Dhahad, H. A., Sharma, K., ABo-Khalil, A. G., El-Shafay, A. S., & Ibrahim, B. F. (2022). Comparative thermoeconomic and thermodynamic analyses and optimization of an innovative solar-driven trigeneration system with carbon dioxide and nitrous oxide working fluids. *Journal of Building Engineering*, 45, 103486.
25. Jeyapaul R, Shahabudeen P, Krishnaiah K. Quality management research by considering multi-response problems in the Taguchi method - A review. *Int J Adv Manuf Technol.* 2005;26(11-12):1331-1337.
26. Kecman V. *Learning and Soft Computing: Support Vector Machines, Neural Networks, and Fuzzy Logic Models.* MIT press; 2001.
27. Oraon M, Sharma V. Prediction of surface roughness in single point incremental forming of AA3003-O alloy using artificial neural network. *Int J Mater Eng Innov.* 2018;9(1):1-19.
28. Al-Muntaser, A. A., Pashameah, R. A., Sharma, K., Alzahrani, E., & Tarabiah, A. E. (2022). Reinforcement of structural, optical, electrical, and dielectric characteristics of CMC/PVA based on GNP/ZnO hybrid nanofiller: nanocomposites materials for energy-storage applications. *International Journal of Energy Research*, 46(15), 23984-23995.
29. Mulay A, Ben S, Ismail S. Artificial Neural Network Modeling of Quality Prediction of a Single Point Incremental Sheet Forming Process. 2017;(June 2018):244-250.
30. Harfoush A, Haapala KR, Tabei A. Application of artificial intelligence in incremental sheet metal forming: A review. *Procedia Manuf.* 2021;53(2020):606-617.
31. Oraon M, Sharma V. Application of artificial neural network: A case of single point incremental forming (SPIF) of Cu67Zn33 alloy. *Manag Prod Eng Rev.* 2021;12(1):17-23.
32. Pepelnjak T, Sevšek L, Lužanin O, Milutinović M. Finite Element Simplifications and Simulation Reliability in Single Point Incremental Forming. *Materials (Basel).* 2022;15(10):3707.